

## Magnetic field-tuned localization of the 5 *f*-electrons in URu<sub>2</sub>Si<sub>2</sub>

N. Harrison,<sup>1</sup> P. J. W. Moll,<sup>2</sup> S. E. Sebastian,<sup>3</sup> L. Balicas,<sup>4</sup> M. M. Altarawneh,<sup>5</sup> J.-X. Zhu,<sup>1</sup> P. H. Tobash,<sup>1</sup> F. Ronning,<sup>1</sup> E. D. Bauer,<sup>1</sup> and B. Batlogg<sup>2</sup>

<sup>1</sup>*Los Alamos National Laboratory, MS E536, Los Alamos, New Mexico 87545, USA*

<sup>2</sup>*Laboratory for Solid State Physics, ETH Zürich, Schafmattstr. 16, CH-8093 Zürich, Switzerland*

<sup>3</sup>*Cavendish Laboratory, Cambridge University, JJ Thomson Avenue, Cambridge CB3 0HE, United Kingdom*

<sup>4</sup>*National High Magnetic Field Laboratory, East Paul Dirac Drive, Tallahassee, Florida 32310, USA*

<sup>5</sup>*Department of Physics, Mu'tah University, Mu'tah, Karak, 61710, Jordan*

(Received 30 September 2013; published 20 December 2013)

We report Shubnikov-de Haas oscillation measurements within the high magnetic field ( $\mu_0 H > 39$  T) magnetically polarized regime of URu<sub>2</sub>Si<sub>2</sub>, made possible using mesoscopic samples prepared by means of focused ion beam lithography. A significant change in the Fermi surface topology relative to the “hidden-order” phase is observed, signaling a transformation into a high magnetic field regime in which 5 *f*-electrons are removed from the Fermi surface. URu<sub>2</sub>Si<sub>2</sub> is therefore a rare example of an actinide compound in which a transformation of 5 *f*-electrons can be directly observed at low temperatures, setting the stage for the unconventional ordering and high magnetic field quantum criticality in this material.

DOI: [10.1103/PhysRevB.88.241108](https://doi.org/10.1103/PhysRevB.88.241108)

PACS number(s): 71.18.+y, 71.27.+a, 71.45.Lr, 75.30.Ds

Strongly renormalized quasiparticle effective masses (i.e., heavy fermions), competing magnetic phases and unconventional superconductivity<sup>1–5</sup> are common to rare-earth and actinide compounds. Yet despite 4 *f*- and 5 *f*-electron systems both lying close to a threshold between itinerant and localized behavior, only the former has revealed clear experimental signatures of such a threshold at low temperatures. Rare-earth compounds provide several examples of a change in Fermi surface volume<sup>6,7</sup> associated with a transformation of 4 *f*-electrons between itinerant and localized 4 *f*-electron behavior tuned by pressure or magnetic field. Meanwhile, no such transformation has been observed in the case of actinide compounds. So, whereas 4 *f*-electrons have been shown by experiment to be readily localized (i.e., removed from the Fermi surface volume) by a uniform magnetic field or antiferromagnetic Weiss field,<sup>8–11</sup> 5 *f*-electrons have thus far been reported to remain itinerant under equivalent conditions.<sup>12,13</sup>

In this Rapid Communication, we show URu<sub>2</sub>Si<sub>2</sub><sup>14</sup> to be an example of a system in which 5 *f*-electrons can be tuned between itinerant and localized electronic configurations by a magnetic field (applied along the crystalline *c* axis at low temperatures). We report magnetic quantum oscillations within the magnetically polarized regime beyond  $\approx 39$  T, revealing greatly reduced effective masses and increased Fermi velocities relative to the low magnetic field regime. The resemblance in behavior to rare-earth systems in which the 4 *f*-electrons are removed from the Fermi surface volume,<sup>8,11,15</sup> suggests that 5 *f*-electrons are being similarly removed from the Fermi surface at magnetic fields above  $\approx 39$  T in URu<sub>2</sub>Si<sub>2</sub>. We discuss the likely impact of a transformation in the behavior of the 5 *f*-electrons on the magnetic ordering in this system<sup>16</sup> and reports of quantum criticality.<sup>17</sup>

Itinerant behavior of the 5 *f*-electrons at low magnetic fields within the hidden-order (HO) phase is suggested by moderately heavy effective masses (ranging from 8 to 25  $m_e$ , where  $m_e$  is the free electron mass)<sup>18–22</sup> and by the similarity of the observed Fermi surface cross-sections to those obtained from band-structure calculations in which the 5 *f*-electrons are treated as band electrons<sup>23,24</sup> (on assuming the hidden order

to be accompanied by unit cell doubling so as to produce a simple tetragonal structure). Owing to a 10<sup>4</sup>-fold reduction in resistivity within the magnetically polarized regime of URu<sub>2</sub>Si<sub>2</sub> at high magnetic fields,<sup>18,19</sup> magnetic quantum oscillation measurements have thus far been restricted to magnetic fields below  $\approx 39$  T.

The key experimental advance enabling us to observe quantum oscillations within the high magnetic field regime here is the utilization of focused ion beam (FIB) lithography for magnetotransport measurements.<sup>25</sup> FIB lithography enables the preparation of mesoscopic samples (see Fig. 1),<sup>25</sup> with which higher signal-to-noise resistivity measurements are possible than on larger single crystals under similar experimental conditions. A large single crystal of URu<sub>2</sub>Si<sub>2</sub> is grown using the Czochralski technique and purified by electrorefinement.<sup>19</sup> FIB lithography is then used to cut a meandering current path of width  $\approx 2$   $\mu\text{m}$  and total length  $\approx 300$   $\mu\text{m}$  in a  $\approx 2$ - $\mu\text{m}$ -thick slab, to which electrical contacts are applied. The general form of the magnetoresistance through the field-induced metamagnetic transitions [between 35 and 38 T in Fig. 1(a)] and the temperature-dependent negative magnetoresistance within the high magnetic field regime [see Fig. 1(c)] are similar to those measured on samples of significantly larger size,<sup>17,18,19</sup> suggesting that use of FIB lithography does not prohibitively degrade the sample quality.

Magnetic quantum oscillations of size  $\sim 10^3$  times smaller than the background resistance [see Fig. 2(a)] become clearly visible after subtracting a background polynomial fit. Oscillatory fits [see Fig. 2(b)] to the background-subtracted data (complemented by Fourier analysis) reveal the presence of multiple quantum oscillation frequency components periodic in inverse magnetic field. The association of the spectral features with distinct cross-sections of Fermi surface is suggested by the absence of harmonic ratios between the frequency values [see Fig. 3(a) and Table I] and by the different values of the fitted quasiparticle effective mass [see Fig. 3(b) and Table I].

Two observations indicate the high magnetic field electronic structure in URu<sub>2</sub>Si<sub>2</sub> (i.e.,  $\mu_0 H > 39$  T) to be different from

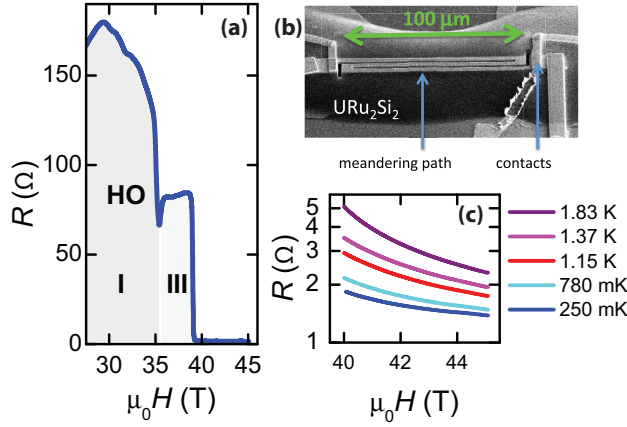


FIG. 1. (Color online) (a) The measured resistance of the FIB-cut  $\text{URu}_2\text{Si}_2$  crystal, showing a precipitous drop on entering the high magnetic field regime above  $\approx 39$  T<sup>19</sup> after exiting hidden order (HO) phase I (and III<sup>17</sup>). (b) An electron micrograph of the FIB-ed crystal. (c) An expanded view of the resistance measured in the high magnetic regime using currents as low as  $30 \mu\text{A}$  at different temperatures ( $T$ ). The resistance varies quadratically with  $T$ , providing a secondary *in situ* temperature calibration.

that within the hidden-order phase at low magnetic fields. First, two of the observed frequencies ( $F_3$  and  $F_4$ ) are significantly

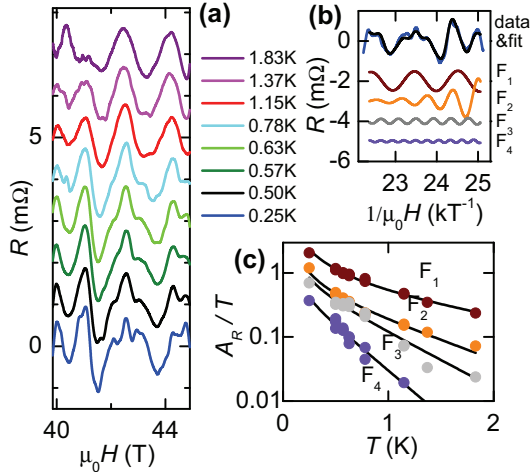


FIG. 2. (Color online) (a) The oscillatory component of the resistance of the FIB-cut  $\text{URu}_2\text{Si}_2$  crystal shown in Fig. 1 at several different temperatures (as indicated) after subtraction of a background polynomial. Multiple sweeps are averaged at the lowest temperature while larger currents ( $I \geq 100 \mu\text{A}$ ) are used at higher temperatures. (b) A fit (black line) of  $A = \sum_i A_i \cos(2\pi F_i/B + \phi_i) \exp(-\Gamma_i/B)$  to the lowest  $T$  data (blue line), where  $B = \mu_0 H$  and where  $F_i$  corresponds to each of the four frequencies ( $F_1$ ,  $F_2$ ,  $F_3$ , and  $F_4$ , confirmed present in Fourier transforms and listed in Table I).  $A_i$  are the amplitude prefactors,  $\phi_i$  are phase factors and  $\Gamma_i$  account for possible field dependencies of the amplitudes. All of the oscillation amplitudes depend weakly on  $B$  with the exception of  $F_2$ , suggesting a possible beat between closely-spaced frequencies. Also shown (in different colors) are the individual contributions to the fit from each of the frequencies. (c) Fits of  $A_R/T$  (where  $A_R$  is the Fourier amplitude) to the Lifshitz-Kosevich term  $A_i / \sinh(2\pi^2 k_B m_i^* T / \hbar e \mu_0 H)$ ,<sup>32</sup> yielding effective masses ( $m_i^*$ ) tabulated in Table I.

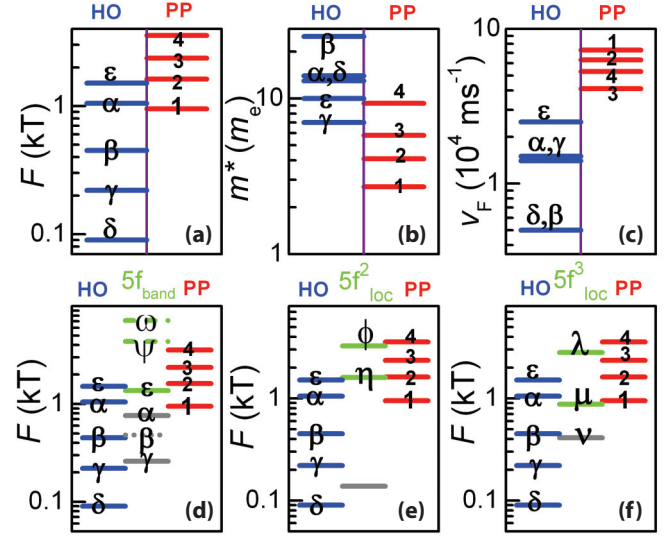


FIG. 3. (Color online) (a), (b), and (c) A comparison between the HO and polarized paramagnetic (PP) regimes of the frequencies ( $F$ ), effective masses ( $m^*$ ), and Fermi velocities ( $v_F$ ) listed in Table 1. The PP regime corresponds to  $\mu_0 H > 38$  T. (d), (e), and (f) A comparison of the quantum oscillation frequencies in the HO and PP regimes with the results of band-structure calculations<sup>24</sup> in which (d) the  $5f$ -electrons are completely itinerant, (e) two  $5f$ -electrons are confined to the atomic core, and (f) three  $5f$ -electrons are confined to the atomic core. Calculated frequencies that are too low to be resolved at high magnetic fields (due to the limited range in  $1/H$ ) are depicted in grey.

larger than those ( $\delta$ ,  $\gamma$ ,  $\beta$ ,  $\alpha$  and  $\epsilon$ ) measured at low magnetic fields within the hidden-order phase.<sup>18–22</sup> Second, the values of the effective masses are seen to be lighter than those measured at low magnetic fields.  $\text{URu}_2\text{Si}_2$  can therefore be seen to behave differently from other superconducting uranium compounds in which quantum oscillations are observed both above and below a metamagnetic transition.<sup>12,13</sup> In  $\text{UPt}_3$ , for example, the effective masses reported at magnetic fields above the metamagnetic transition ( $H_m \approx 20$  T) are similarly heavy to those at low magnetic fields,<sup>12</sup> suggesting that the  $5f$ -electrons

TABLE I. Tabulated values of the measured frequency  $F_i$ , the fitted effective mass  $m_i^*$  and the orbitally averaged Fermi velocity  $v_{F,i} = \sqrt{2e\hbar F_i/m^*}$ . The larger uncertainty in  $F_1$  compared to the higher frequencies results from the small number ( $\approx 3$ ) of oscillations. In the last five rows, we list the frequencies reported within the HO phase.<sup>19,22</sup>

orbit	$F_i$ (T)	$m_i^*$ ( $m_e$ )	$v_{F,i}$ ( $10^4$ m/s)
$F_1$	950(50)	2.7(3)	7.3
$F_2$	1620(10)	4.1(5)	6.3
$F_3$	2360(10)	5.8(7)	5.3
$F_4$	3560(10)	9.3(9)	4.1
$\delta$	90	13	0.5
$\gamma$	220	7	1.4
$\beta$	450	25	0.5
$\alpha$	1050	14	1.5
$\epsilon$	1510	10	2.5

continue to contribute significantly to the quasiparticle bands in that system despite their partial polarization by a magnetic field. A similar behavior prevails in UPd<sub>2</sub>Al<sub>3</sub> (for which  $H_m \approx 18$  T),<sup>13</sup> although only two frequencies are observed. By contrast, all of the effective masses observed above the metamagnetic transitions (occurring between 35 and 39 T) in URu<sub>2</sub>Si<sub>2</sub> are less than  $10 m_e$ . A reduction in the strength of electronic correlations must therefore occur in URu<sub>2</sub>Si<sub>2</sub> at high magnetic fields, which may then further explain the previously observed reduction in the electronic heat capacity within the high magnetic field regime.<sup>26</sup>

The transformation in Fermi surface in URu<sub>2</sub>Si<sub>2</sub> becomes particularly striking on considering the orbitally averaged Fermi velocity  $v_{F,i} = \sqrt{2e\hbar F_i/m^*}$ , which enables the relative slopes of the electronic dispersions at the Fermi surface to be compared. Whereas velocities within the low magnetic field HO phase of URu<sub>2</sub>Si<sub>2</sub> lie in the range  $0.5$  to  $2.5 \times 10^4$  ms<sup>-1</sup>, those within the high magnetic field regime above 39 T lie between  $4$  and  $7 \times 10^4$  ms<sup>-1</sup>. Hence there is a roughly fourfold increase in Fermi velocity on entering the high magnetic field regime of URu<sub>2</sub>Si<sub>2</sub>, indicating the 5*f*-electron contribution to the Fermi surface to be greatly reduced. By contrast, the Fermi velocities of UPt<sub>3</sub> at high magnetic fields, which lie in the range  $0.3$  to  $1.6 \times 10^4$  ms<sup>-1</sup>,<sup>12</sup> are roughly seven times lower than those detected in URu<sub>2</sub>Si<sub>2</sub> at high magnetic fields. Meanwhile, the two high magnetic field Fermi velocities of UPd<sub>2</sub>Al<sub>3</sub>, namely  $1.1$  and  $4.3 \times 10^4$  ms<sup>-1</sup>,<sup>13</sup> lie between those observed in URu<sub>2</sub>Si<sub>2</sub> and UPt<sub>3</sub>.

Thus, while the quasiparticles remain heavy and slow at magnetic fields above the metamagnetic transitions in UPt<sub>3</sub> and UPd<sub>2</sub>Al<sub>3</sub>, as might be expected for partially polarized narrow 5*f*-electron bands, the values of the effective masses and Fermi velocities observed at high magnetic fields in URu<sub>2</sub>Si<sub>2</sub> are similar to those seen in rare earth systems in which the 4*f*-electrons are removed from the Fermi surface.<sup>8,11,15,27</sup> URu<sub>2</sub>Si<sub>2</sub> therefore appears to be an actinide compound in which 5*f*-electrons are removed from the Fermi surface in strong magnetic fields. Comparisons of the observed frequencies in URu<sub>2</sub>Si<sub>2</sub> at high magnetic fields with those predicted by itinerant and localized 5*f*-electron band-structure calculations in Figs. 3(d)–3(f) support such a hypothesis. Band structure calculations in which two or three 5*f*-electrons are confined to the atomic core [corresponding to the 5*f*<sup>2</sup> and 5*f*<sup>3</sup> electronic configurations in Figs. 3(e), 3(f), and 5] can explain some of the experimental frequencies. The doubling of the number of frequencies observed in the experiment is likely to be associated with nonlinear Zeeman splitting of the quasiparticle bands.

By contrast, poor agreement can be seen between the high magnetic field experimental frequencies and itinerant 5*f*-electron band structure calculations [see Fig. 3(d)]. Were the 5*f*-electrons to remain itinerant at high magnetic fields where the hidden-order phase<sup>17</sup> and field-induced phases<sup>16</sup> are destroyed, one would expect an unreconstructed Fermi surface upon closure of the hidden-order gap. Two main observations would be associated with an unreconstructed Fermi surface in the original body-centered tetragonal Brillouin zone: (i) persistence of low frequencies (i.e.,  $\delta$ ,  $\gamma$ ,  $\alpha$ , and  $\epsilon$ <sup>24</sup>) that are unaffected by folding of the Brillouin zone and (ii) appearance

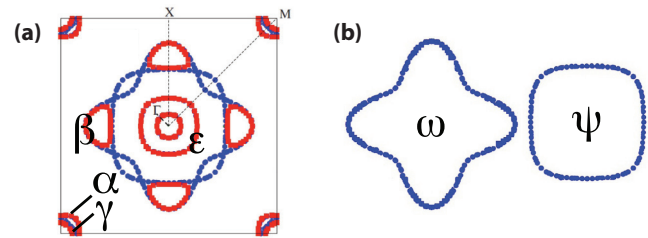


FIG. 4. (Color online) (a) Reconstruction of the Fermi surface according to Oppeneer *et al.*,<sup>24</sup> resulting in the creation of small pockets labeled  $\beta$ . (b) The larger unreconstructed Fermi surface pockets of Oppeneer *et al.*<sup>24</sup> expected in the original body-centered tetragonal Brillouin zone.

of two larger frequencies [i.e.,  $\omega$  and  $\psi$  in Figs. 3(d) and 4]. Neither (i) or (ii) appear to be supported by the experimental data.

When a transformation in the *f*-electrons between itinerant and localized behavior occurs, it strongly influences the nature of the magnetic ordering at low temperatures.<sup>16</sup> On evaluating the Zeeman energy  $h \approx \frac{g^*}{2} \mu_B \mu_0 H \approx 2.9$  meV (where  $g^* \approx 2.6$  is the experimentally determined effective *g* factor<sup>28</sup> for the field along the *c* axis and  $\mu_0 H \approx 39$  T) that is required to remove the 5*f*-electrons from the Fermi surface, we find it to be comparable to the magnitude of the hidden-order parameter  $\Delta_{HO} \approx 2.5$  meV estimated from scanning tunneling microscopy measurements.<sup>29</sup> The similarities in energy and field at which the hidden-order transition<sup>16,17</sup> and Fermi surface transformation between localized and itinerant behavior occur suggest that these two phenomena cannot be considered independently. Previous reports of quantum critical behavior at  $\approx 37$  T<sup>17</sup> suggest its connection to the coupling between 5*f*-electrons and conduction electrons, as is also thought to be the case in the 4*f*-electron systems CeRhIn<sub>5</sub><sup>7</sup> and YbRh<sub>2</sub>Si<sub>2</sub>.<sup>6</sup> One important difference in URu<sub>2</sub>Si<sub>2</sub>, however, is that the hidden magnetic order (which forms below  $T_{HO} \approx 17.5$  K<sup>16</sup>) occurs in conjunction with itinerant *f*-electron behavior rather than localized *f*-electron behavior. The coexistence of itinerant behavior with the hidden-order phase lends support to the notion of a “hybridization order parameter” in URu<sub>2</sub>Si<sub>2</sub>.<sup>30,31</sup>

In summary, we report Shubnikov-de Haas oscillation measurements within the high magnetic field magnetically

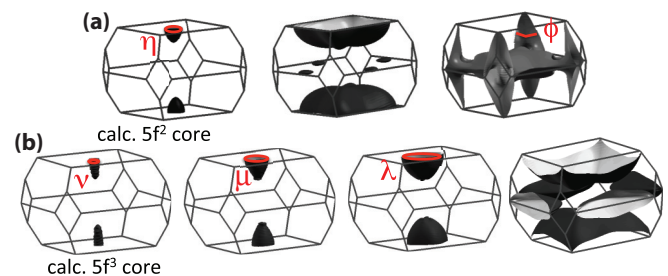


FIG. 5. (Color online) (a) and (b) Predicted sheets of Fermi surface of URu<sub>2</sub>Si<sub>2</sub> in which two or three 5*f*-electrons are confined to the atomic core, respectively. Each has two extremal cross-sections for  $H \parallel \hat{c}$  that are comparable to frequencies observed at high magnetic fields [see Figs. 3(e) and 3(f)].

polarized regime of URu<sub>2</sub>Si<sub>2</sub>, made possible using mesoscopic samples prepared by means of FIB lithography. A significant change in the Fermi surface topology relative to the hidden-order phase is evidenced at magnetic fields above  $\approx 39$  T by the observation of larger frequencies, lighter effective masses and greatly increased Fermi velocities, which are consistent with the removal of  $5f$ -electrons from the Fermi surface. Such an observation is presently unique among actinide materials, pointing to a fundamental transformation in Fermi surface being an important factor in the high magnetic field quantum critical behavior<sup>17</sup> and unconventional ordering, for which this materials has become well known.<sup>16</sup>

N.H. and M.M.A.s acknowledge the provision of the US Department of Energy (DOE), Office of Basic Energy Sciences (BES) funding for the “Science of 100 Tesla.” M.M.A. further acknowledges a Seaborg fellowship. L.B. is supported by DOE-BES through award DE-SC0002613. Work by P.H.T., F.R., and E.D.B. is supported by the US DOE, Office of BES, MSE Division and by the LANL LDRD program. S.E.S. acknowledges the Royal Society. Experiments were performed at the NHMFL, which is supported by the US DOE, the National Science Foundation and the State of Florida. N.H. thanks P. Oppeneer for providing cross-sections of the calculated Fermi surface. Electron microscopy and FIB work was performed at the Electron Microscopy group ETH Zürich (EMEZ).

- <sup>1</sup>A. C. Hewson, *The Kondo Problem to Heavy Fermions* (Cambridge University Press, Cambridge 1993).
- <sup>2</sup>N. D. Mathur, F. M. Grosche, S. R. Julian, I. R. Walker, D. M. Freye, R. K. W. Haselwimmer, and G. G. Lonzarich, *Nature (London)* **394**, 39 (1998).
- <sup>3</sup>Q.-M. Si, S. Rabello, K. Ingersent, J. L. Smith, *Nature (London)* **413**, 804 (2001).
- <sup>4</sup>J. L. Sarrao, L. A. Morales, J. D. Thompson, B. L. Scott, G. R. Stewart, F. Wastin, J. Rebizant, P. Boulet, E. Colineau, and H. H. Lander, *Nature (London)* **420**, 297 (2002).
- <sup>5</sup>H. von Loehneysen, A. Rosch, M. Vojta, and P. Wolfle, *Rev. Mod. Phys.* **79**, 1015 (2007).
- <sup>6</sup>J. Custers, P. Gegenwart, H. Wilhelm, K. Neumaier, Y. Tokiwa, O. Trovarelli, C. Geibel, F. Steglich, C. Pepin, and P. Coleman, *Nature (London)* **424**, 524 (2003).
- <sup>7</sup>T. Park, F. Ronning, H.-Q. Yuan, M. B. Salamon, R. Movshovich, J. L. Sarrao, and J. D. Thompson, *Nature (London)* **440**, 65 (2006).
- <sup>8</sup>H. Aoki, S. Uji, A. K. Albessard, and Y. Onuki, *Phys. Rev. Lett.* **71**, 2110 (1993).
- <sup>9</sup>H. Shishido, R. Settai, H. Harima, and Y. Onuki, *J. Phys. Soc. Jpn.* **74**, 1103 (2005).
- <sup>10</sup>R. Settai, T. Kubo, T. Shiromoto, D. Honda, H. Shishido, K. Sugiyama, Y. Haga, T. D. Matsuda, K. Betsuyaku, H. Harima, T. C. Kobayashi, and Y. Onuki, *J. Phys. Soc. Jpn.* **74**, 3016 (2005).
- <sup>11</sup>N. Harrison, S. E. Sebastian, C. H. Mielke, A. Paris, M. J. Gordon, C. A. Swenson, D. G. Rickel, M. D. Pacheco, P. F. Ruminer, J. B. Schillig, J. R. Sims, A. H. Lacerda, M. T. Suzuki, H. Harima, and T. Ebihara, *Phys. Rev. Lett.* **99**, 056401 (2007).
- <sup>12</sup>S. R. Julian, P. A. A. Teunissen, and S. A. J. Wieggers, *Phys. Rev. B* **46**, 9821 (1992).
- <sup>13</sup>T. Terashima, C. Haworth, M. Takashita, H. Aoki, N. Sato, and T. Komatsubara, *Phys. Rev. B* **55**, R13369 (1997).
- <sup>14</sup>T. M. Palstra, A. A. Menovsky, J. van den Berg, A. J. Dirkmaat, P. H. Kes, G. J. Nieuwenhuys, and J. A. Mydosh, *Phys. Rev. Lett.* **55**, 2727 (1985).
- <sup>15</sup>M. M. Altarawneh, N. Harrison, R. D. McDonald, F. F. Balakirev, C. H. Mielke, P. H. Tobash, J.-X. Zhu, J. D. Thompson, F. Ronning, and E. D. Bauer, *Phys. Rev. B* **83**, 081103 (2011).
- <sup>16</sup>J. A. Mydosh and P. M. Oppeneer, *Rev. Mod. Phys.* **83**, 1301 (2011).
- <sup>17</sup>K.-H. Kim, N. Harrison, M. Jaime, G. S. Boebinger, and J. A. Mydosh, *Phys. Rev. Lett.* **91**, 256401 (2003).
- <sup>18</sup>Y. J. Jo, L. Balicas, C. Capan, K. Behnia, P. Lejay, J. Flouquet, J. A. Mydosh, and P. Schlottmann, *Phys. Rev. Lett.* **98**, 166404 (2007).
- <sup>19</sup>M. M. Altarawneh, N. Harrison, S. E. Sebastian, L. Balicas, P. H. Tobash, J. D. Thompson, F. Ronning, and E. D. Bauer, *Phys. Rev. Lett.* **106**, 146403 (2011).
- <sup>20</sup>C. Bergemann, S. R. Julian, G. J. McMullan, B. K. Howard, G. G. Lonzarich, P. Lejay, J. P. Brison, and J. Flouquet, *Physica B* **230**, 348 (1997).
- <sup>21</sup>H. Ohkuni, Y. Inada, Y. Tokiwa, K. Sakurai, R. Settai, T. Honma, Y. Haga, E. Yamamoto, Y. Onuki, H. Yamagami, S. Takahashi, and T. Yanagisawa, *Philos. Mag. B* **79**, 1045 (1999).
- <sup>22</sup>E. Hassinger, G. Knebel, T. D. Matsuda, D. Aoki, V. Taufour, and J. Flouquet, *Phys. Rev. Lett.* **105**, 216409 (2010).
- <sup>23</sup>H. Yamagami and N. Hamada, *Physica B* **284**, 1295 (2000).
- <sup>24</sup>P. M. Oppeneer, J. Ruzs, S. Elgazzar, M. T. Suzuki, T. Durakiewicz, and J. A. Mydosh, *Phys. Rev. B* **82**, 205103 (2010).
- <sup>25</sup>P. J. W. Moll, R. Puzniak, F. Balakirev, K. Rogacki, J. Karpinski, N. D. Zhigadlo, and B. Batlogg, *Nat. Mater.* **9**, 628 (2010).
- <sup>26</sup>M. Jaime, K. H. Kim, G. Jorge, S. McCall, and J. A. Mydosh, *Phys. Rev. Lett.* **89**, 287201 (2002).
- <sup>27</sup>U. Alver, R. G. Goodrich, N. Harrison, D. W. Hall, E. C. Palm, T. P. Murphy, S. W. Tozer, P. G. Pagliuso, N. O. Moreno, J. L. Sarrao, and Z. Fisk, *Phys. Rev. B* **64**, 180402 (2001).
- <sup>28</sup>M. M. Altarawneh, N. Harrison, G. Li, L. Balicas, P. H. Tobash, F. Ronning, and E. D. Bauer, *Phys. Rev. Lett.* **108**, 066407 (2012).
- <sup>29</sup>A. R. Schmidt, M. H. Hamidian, P. Wahl, F. Meier, A. V. Balatsky, J. D. Garrett, T. J. Williams, G. M. Luke, and J. C. Davis, *Nature (London)* **465**, 570 (2010); P. Aynajian, E. H. D. Neto, C. V. Parker, Y. K. Huang, A. Pasupathy, J. A. Mydosh, and A. Yazdani, *Proc. Natl. Acad. Sci. USA* **107**, 10383 (2010).
- <sup>30</sup>Y. Dubi and A. V. Balatsky, *Phys. Rev. Lett.* **106**, 086401 (2011).
- <sup>31</sup>P. Chandra, P. Coleman, and R. Flint, *Nature (London)* **493**, 621 (2013).
- <sup>32</sup>D. Shoenberg, *Magnetic Oscillations in Metals* (Cambridge University Press, Cambridge 1984).